




Review

Exploring the Origin of the Two-Week Predictability Limit: A Revisit of Lorenz's Predictability Studies in the 1960s

Bo-Wen Shen ^{1,*} , Roger A. Pielke, Sr. ², Xubin Zeng ³  and Xiping Zeng ⁴ ¹ Department of Mathematics and Statistics, San Diego State University, San Diego, CA 92182, USA² Cooperative Institute for Research in Environmental Sciences, University of Colorado Boulder, Boulder, CO 80203, USA; pielkesr@gmail.com³ Department of Hydrology and Atmospheric Science, The University of Arizona, Tucson, AZ 85721, USA; xubin@arizona.edu⁴ DEVCOM Army Research Laboratory, Adelphi, MD 20783, USA; xiping.zeng.civ@army.mil

* Correspondence: bshen@sdsu.edu

Abstract: The 1960s was an exciting era for atmospheric predictability research: a finite predictability of the atmosphere was uncovered using Lorenz's models and the well-acknowledged predictability limit of two weeks was estimated using a general circulation model (GCM). Here, we delve into details regarding how a correlation between the two-week predictability limit and a doubling time of five days was established, recognize Lorenz's pioneering work, and suggest non-impossibility for predictability beyond two weeks. We reevaluate the outcomes of three different approaches—dynamical, empirical, and dynamical-empirical—presented in Lorenz's and Charney et al.'s papers from the 1960s. Using the intrinsic characteristics of the irregular solutions found in Lorenz's studies and the dynamical approach, a doubling time of five days was estimated using the Mintz–Arakawa model and extrapolated to propose a predictability limit of approximately two weeks. This limit is now termed “Predictability Limit Hypothesis”, drawing a parallel to Moore's Law, to recognize the combined direct and indirect influences of Lorenz, Mintz, and Arakawa under Charney's leadership. The concept serves as a bridge between the hypothetical predictability limit and practical model capabilities, suggesting that long-range simulations are not entirely constrained by the two-week predictability hypothesis. These clarifications provide further support to the exploration of extended-range predictions using both partial differential equation (PDE)-physics-based and Artificial Intelligence (AI)—powered approaches.

Keywords: predictability limit; chaos; Lorenz models; doubling time; extended-range predictions; general circulation model



Citation: Shen, B.-W.; Pielke, R.A., Sr.; Zeng, X.; Zeng, X. Exploring the Origin of the Two-Week Predictability Limit: A Revisit of Lorenz's Predictability Studies in the 1960s. *Atmosphere* **2024**, *15*, 837. <https://doi.org/10.3390/atmos15070837>

Academic Editor: Jordan G. Powers

Received: 28 May 2024

Revised: 23 June 2024

Accepted: 3 July 2024

Published: 16 July 2024



Copyright: © 2024 by the authors. Licensee MDPI, Basel, Switzerland. This article is an open access article distributed under the terms and conditions of the Creative Commons Attribution (CC BY) license (<https://creativecommons.org/licenses/by/4.0/>).

1. Introduction

Although a predictability limit of approximately two weeks for weather is widely acknowledged, there is ongoing exploration regarding the feasibility of subseasonal-to-seasonal (S2S) predictions (e.g., National Academies, 2020 [1]), encompassing timeframes from two weeks to several months using both partial differential equation (PDE)-physics-based and AI-powered approaches. The significance of S2S predictions is widely recognized in various domains, including in agriculture, water resources, emergency management, energy, aviation, and maritime planning (National Research Council [2]; National Academies, 2016 [3]). Nevertheless, the feasibility of S2S predictions may require better understanding of the meaning of the conventional two-week predictability limit.

Since the 1960s, we have observed the advance of both numerical models and data assimilation systems that collectively produce promising, long-range simulations over two weeks (e.g., Sonechkin et al. 1995; Mukougawa et al., 2005; Shen et al., 2010, 2011; Shen 2019b; Krishnamurthy and Sharma 2017; Krishnamurthy 2019; Judt 2018, 2020 [4–12]). Such advances create a gap between the well-acknowledged two-week predictability limit and the practical capabilities of models, necessitating a reevaluation of the two-week limit.

Our study is not focused on establishing a theoretical foundation for S2S predictions. Instead, we reassess the genesis of the two-week limit and clarify some misunderstanding regarding the limit by revisiting predictability studies conducted during the early phase of the Global Atmospheric Research Program (GARP) in the 1960s. We then present further insights to mitigate the constraints imposed on S2S predictions by this limit. The forthcoming discussion will encompass findings indicating that the determination of the two-week limit lacked robustness during the 1960s and that the definition of the predictability limit has since evolved.

To provide a foundation for subsequent discussions, we first provide Lorenz’s updated perspective on predictability limits from the 1990s and 2000s by summarizing the recent study of Shen et al. (2023b [13]) who reviewed relevant literature, including Lorenz (1993) [14] and Reeves (2014) [15]. Lorenz’s updated perspective, as outlined in Table 1, indicates that while the concept of finite predictability was suggested by Lorenz’s models, the two-week predictability limit was established during the 1960s using a doubling time of five days based on a General Circulation Model (GCM). A doubling time of five days implies that small errors typically take approximately five days to double. While the findings in Table 1 that are supported by our recent papers are summarized below, the new insights of the Lorenz 1963 and 1969 models are presented in Section 2.

Table 1. Important concepts for predictability limits.

	Contents	References
Lorenz’s View	<ul style="list-style-type: none"> A. The Lorenz 1963 model qualitatively revealed the essence of finite predictability within a chaotic system, such as the atmosphere. However, the Lorenz 1963 model did not determine a precise limit for atmospheric predictability. B. During the 1960s, using real-world models, the two-week predictability limit was originally estimated based on a doubling time of five days. Since then, this finding has been documented in Charney et al. (1966) [16] and has become a consensus. 	Shen et al. (2023b, 2022a [13,17])
Predictability Limit Hypothesis	<ul style="list-style-type: none"> • Much like Moore’s Law in the realm of computing, the Predictability Limit Hypothesis, specifically the two-week predictability limit, is an empirical association based on practical modeling and idealized chaotic modeling from the 1960s. It stands as a limited set of observed findings and as a reasonable extrapolation from early modeling results in the 1960s, rather than constituting fundamental physics. 	Concluding remarks in this study

Although a doubling time was used to estimate the predictability limit during the 1960s and in subsequent years, other time scales have been applied for predictability estimates using real-world and/or theoretical models. As summarized in Table 2, various definitions of predictability include use of the saturation time, Lyapunov exponent, and anomaly correlation coefficients (ACC). The doubling and saturation times are illustrated in the Supplementary Materials.

Table 2. Various time scales and concepts for predictability estimates.

Term		Remarks
Doubling time	The doubling time (or e-folding time) represents the time for a specific mode with a growth rate to increase by a factor of 2 (or e).	Charney et al. (1966) [16]
Saturation time	Saturation time is defined as the time for the perturbation (e.g., root-mean square error) to become saturated (i.e., reaching a time-independent constant).	Lorenz (1969d) [18]
Turnover time (τ_k)	Turnover time represents the time for a parcel with velocity v_k to move a distance of $1/k$, with v_k being the velocity associated with wavenumber k . The turnover time is further used to indicate the time that an error at one wavenumber spreads to another wavenumber, a movement within the spectral space.	Vallis (2006) [19]; Lloveras et al. (2022) [20]

Table 2. Cont.

Term		Remarks
Lyapunov exponent	A global Lyapunov exponent represents the long-term average of local growth rates that vary with time. Its reciprocal indicates the time scale for error growth.	Shen et al. (2022a) [17]
Anomaly correlation coefficients (ACC)	The maximum time duration associated ACC when 0.6 is defined as the predictability limit.	This definition has been used by operational centers for several decades (e.g., Owens and Hewson 2018 [21]; Lin, Shen et al., 2003 [22]).

In regard to the use of a global positive Lyapunov exponent for predictability assessments, as discussed by Shen et al. (2022a) [17] and other researchers, a global Lyapunov exponent is determined by the long-time average of time-varying local Lyapunov exponents (i.e., time-varying local growth rates). As a result, while the existence of a global Lyapunov exponent may imply finite predictability in chaotic systems, its averaged characteristics may not effectively establish an upper limit on predictability (e.g., Lorenz 1996, 2006 [23,24]). See a concise mathematical review in Shen (2024) [25].

In comparison, the current approach for predictability estimates of the real-world models is to use anomaly correlation coefficients (ACC, e.g., Pegion et al., 2019 [26]; Lin et al., 2003 [22]), which are widely used to evaluate AI-powered models as discussed in Section 3.2. Based on the ECMWF Forecast User Guide (Owens and Hewson 2018 [21]), ACC represents “the spatial correlation between a forecast anomaly relative to climatology, and a verifying analysis anomaly relative to climatology.” When the ACC value dips below 0.6, the result suggests that the positioning of synoptic scale features becomes irrelevant for forecasting. Thus, predictability determined by doubling time during the 1960s and by the ACC in recent years should be compared with caution.

The above suggests that the two-week limit determined by a doubling time of 5 days should not be perceived as a definitive ceiling for atmospheric predictability. Such a limit does not inherently establish an upper threshold on the limit estimated by the ACC. To reinforce this idea and to achieve our goals, we (1) provide a historical account of how a doubling time of five days was determined and extrapolate to estimate a predictability limit of two weeks, and (2) propose a concept that acknowledges the direct contribution of the GCM, as well as the indirect influence of Lorenz’s chaotic models, in determining the doubling time and, consequently, the predictability limit. Our work is partly intended as a scientific history for recognizing Lorenz’s pioneering work and as the additional support for exploring atmospheric predictability beyond two weeks using both PDE-physics-based and AI-powered systems.

2. A Review of the Studies in the 1960s for New Insights

During the 1960s, Lorenz published significant papers concerning predictability limits within the atmosphere. Since then, his notable work Lorenz (1963) [27] has garnered substantial citations across various fields (Gleick, 1987 [28]; Stewart (2002) [29]; Lorenz, 1993 [14]) and his study Lorenz (1969d) [18] has been frequently cited in *Meteorology*. In fact, in a single year, 1969, Lorenz published six papers (Lorenz 1969a, b, c, d e, f [18,30–34]). Five of these papers specifically discussed estimations of predictability limits. These five studies from 1969, together with relevant works by Lorenz himself, and other colleagues (such as Charney et al., 1966 [16]; GARP 1969 [35]; Smagorinsky 1969 [36]; Lorenz 1970, 1972, 1984a, 1985 [37–40], 1993 [14]), are revisited and summarized to reiterate the fact that while the 1963 and 1969 models suggest finite predictability, the two-week limit was suggested based on a doubling time of 5 days by Charney et al. (1966) [16].

Below, we reviewed a comprehensive final report by Lorenz for the Air Force Research Laboratories, Office of Aerospace Research (Lorenz 1969a [30], hereafter referred to as L69a), as well as a section on the “theoretical limits of predictability” in Charney et al. (1966) [16]. Our discussions begin with a layout of the L69a report, which consists of the following four parts:

- (1) Three approaches for atmospheric predictability (Lorenz 1969b [31]);
- (2) Atmospheric predictability as indicated by numerical experiments (Charney et al. 1966 [16]);
- (3) Atmospheric predictability as revealed by naturally occurring analogues (Lorenz 1969c [32]);
- (4) The predictability of a flow which possesses many scales of motion (Lorenz 1969d [18]).

The first part (Lorenz 1969b [31]) was published by the Bulletin of the American Meteorological Society (BAMS) and, here, is referred to as the L69 BAMS study. The study summarized the findings of a predictability limit, or a doubling time, using three approaches from three other parts (i.e., Charney et al. 1966 [16]; Lorenz 1969c [32], 1969d [18]). The three approaches are as follows:

- (a) A dynamical approach using atmospheric general circulation models;
- (b) An empirical approach based on natural “analogues”, defined below;
- (c) A dynamical-empirical approach that applied a system of 21, linear, 2nd-order ordinary differential equations (ODEs) with coefficients estimated using an atmospheric kinetic energy spectrum.

The model in the dynamical-empirical approach is the so-called Lorenz 1969 model. The atmospheric kinetic energy spectrum was applied to provide upper bounds in order to constrain unbounded growth in the linear 1969 model, yielding saturation times (as defined in Table 2) over different wavelengths. Over the past 15 years, the Lorenz 1969 model has regained significant attention after recent revisits of, for example, Rotunno and Synder (2008) [41], Durran and Gingrich (2014) [42], Palmer et al. (2014) [43], Sun and Zhang [44] and Shen et al. (2022a,b) [17,45].

We present an overview of findings obtained through the aforementioned approaches, together with insightful comments on these methodologies. For ease of reference and to enable meaningful discussions, seven figures were reproduced or derived from previous studies. Promising simulations reported in Smagorinsky (1969) [36] as well as recent AI-enabled studies are also presented. Comments on doubling times of ~two–three days are additionally provided in the Supplementary Materials.

2.1. The Doubling Time of 5 Days and Its Extrapolation for Two-Week Predictability

In the 1960s, to estimate the predictability limit, the GARP’s panel chaired by Charney conducted numerical experiments using different GCMs. Three models, including the Leith, Mintz–Arakawa, and Smagorinsky models (Leith 1965 [46]; Mintz 1964 [47]; Smagorinsky 1963 [48]), were used for simulations. As discussed, such an approach was referred to as the dynamical approach. As outlined in Figure 1, major findings from the selected GCMs were as follows: (i) no systematic growth rates within the Leith model; (ii) a doubling time of 5 days within the Mintz–Arakawa model; and (iii) a doubling time of 10 days and 6–7 days during the first and second 30 days, respectively, within the Smagorinsky model.

Based on a doubling time of five days from the Mintz–Arakawa model, the panel reached the following conclusion (Charney et al. 1966) [16]:

“We may summarize our results in the statement that, based on the most realistic of the general circulation models available, the limit of deterministic predictability for the atmosphere is about two weeks in the winter and somewhat longer in the summer.”

Subsequently, the above conclusion yielded the following statement:

“the limit of deterministic predictability, i.e., the limit of predictability of synoptic-scale motions, is about 2–3 weeks.”

When queried regarding the foundation for this statement, a report entitled “A Guide to GARP” (GARP 1969) [35] reiterated the conclusion of Charney et al. (1966) [16] by providing the following responses:

“This statement first appeared in the aforementioned report of the NAS/NRC Panel on International Meteorological Cooperation, “The Feasibility of a Global Observation and Analysis Experiment.” It is based on numerical experiments conducted by the Panel with

the use of various general circulation models, particularly the model developed at UCLA by Mintz and Arakawa.”

name	methodology	doubling time	remarks
dynamical	real–world models	S63: 10 days M64: 5 days L65: large	yielding a predictability limit of 2 weeks
empirical	analogues	analogues: 8 days quadratic H: 2.5 days cubic H: 5 days	Lorenz (1969b, BAMS) believed that a reasonable value is 2.5 days
dynamical–empirical	The L69 model + an observed spectrum	5 days using the coefficients compatible to the Arakawa’s scheme in M64	Lorenz (1969b, BAMS) believed that a reasonable value is 2.5 days

S63: Smagorinsky (1963)
M64: Mintz (1964)
L65: Leith (1965)

Note the Lorenz (1969d) study mainly applied a **saturation time** to determine a predictability range, which was not discussed in 1969 BAMS article but in 1996/2006 article.

Figure 1. Three approaches for growth rate estimates; a summary of Lorenz (1969b, c, d, e [18,31–33]).

While the two-week predictability limit was determined using the Mintz–Arakawa model, Arakawa suggested that such a predictability statement has yielded controversy, as documented in Lewis (2005) [49]:

“It showed, for the first time using a realistic model of the atmosphere, the existence of a deterministic predictability limit the order of weeks. The report specifically says that the limit is two weeks, which became a matter of controversy later. To me, there is no reason that it is a fixed number. It should depend on many factors, such as the part of the time/space spectrum, climate and weather regimes, region of the globe and height in the vertical, season, etc.”

Indeed, if we consider a doubling time of five days, reducing initial error amplitudes by half could potentially extend the predictability range by an additional five days. As a result, continuous extensions of predictability horizons become possible by minimizing initial errors [25], aligning with Arakawa’s viewpoint. Further elaboration on determination of the five-day doubling time is provided below.

2.2. A Revisit of the Dynamical Approach in Charney et al. (1966)

In Charney et al. (1966) [16], the section entitled “Theoretical Limits of Predictability” describes numerical experiments conducted with the aforementioned atmospheric GCMs. As reported, the Leith model exhibited a transient oscillation followed by a leveling off for errors, and thus, the model was terminated after 20 days. Errors due to computational instability are associated with the condensation process.

By comparison, the additional two GCMs were run for an extended period (e.g., more than 200 days). Then, an “error” perturbation in the temperature field was introduced, and predictions were made for at least 30 additional days. These predictions were then

compared to the evolution of unperturbed flow over the same period. Errors were determined by the differences in the simulations between unperturbed and perturbed runs. By evaluating the growth rate of errors, representing how fast an error grows at the cost of instability in the state of an unperturbed run, a doubling time was determined.

The Mintz–Arakawa model was integrated for upward of 284 days, with the Sun constantly in the location for the Northern Hemisphere winter solstice. A sequence of sea-level pressure charts for days 229–243 were presented (e.g., Figures 5–8 of Charney et al. 1966) [16]. Error growth was sequentially analyzed, as follows. For the perturbed run, an error was inserted on Day 234, and growth of the root-mean-square (r.m.s. or RMS) temperature error from Day 234 to Day 264 was analyzed. The middle panel of Figure 2 displays an initial decaying error, and then, an exponentially growing rate.

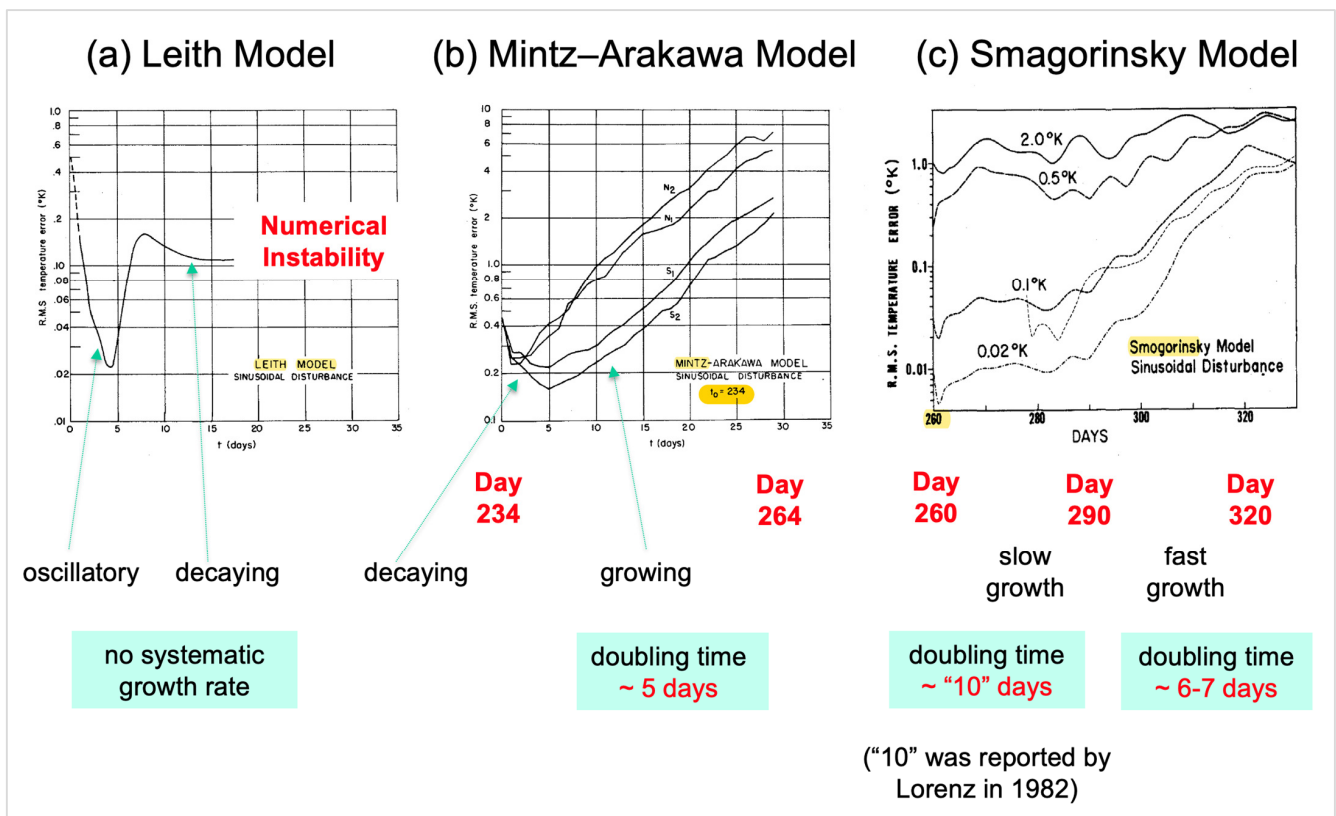


Figure 2. Growth rates in the three models of Charney et al. (1966) [16]. The three panels, from left to right, are from Figures 2, 3, and 4a of Charney et al. (1966) [16], respectively.

A doubling time of five days was estimated using the Mintz–Arakawa model and applied in order to extrapolate a predictability limit of two weeks. On the other hand, as shown on page 212 of Charney (1966) [16], as follows, larger predictability limits (e.g., 26 or 29 days) were also documented in the same report:

“we note that all predictability in the Northern Hemisphere is lost at 26 days for the wave perturbation, 19 days for the random perturbation, and 29 days for the localized perturbation.”

Additionally, following a 233-day simulation, the model should have already developed its own “equilibrium” state, which could not accurately represent the true atmosphere. Otherwise, the 233-day simulation suggested a predictability limit of up to 233 days. Thus, the estimated doubling time is inversely related to the instability of the model’s long-term state (i.e., the state of the model following extensive simulations) rather than the initial atmospheric state. As a result, an estimate for a predictability limit does not necessarily represent the predictability limit of the atmosphere. In comparison, modern data assi-

lation systems (DAS) are capable of producing a model state that realistically represents an atmospheric state. Thus, doubling times determined using the GCM in the 1960s and modern models with DAS should be compared with caution.

The above findings suggest that various predictability limits depend on different types of initial perturbations and the model's long-term states. This dependence is further illustrated below.

The Smagorinsky model also contained multiple experiments, with different types of initial temperature disturbances. The top panel of Figure 4 in Charney et al. (1966) [16] is shown in the right panel of Figure 2, and displays the time evolution of RMS errors for 60 days, from Day 260 to Day 320, for a case with a periodic wave perturbation. Alongside this panel, we analyzed the following excerpt on page 209 of Charney et al. (1966) [16]:

“The smaller error disturbances, of amplitude 0.1°K and 0.02°K , show a slow but continuous growth until after about 30 days, when the doubling time reaches the value of 6 or 7 days. An examination of the actual flow patterns revealed that the motion was primarily periodic, with a small aperiodic component. After about 30 days the vacillating regime changed to a more aperiodic behavior, and at that time the error grew more rapidly with a doubling time of 6 or 7 days. This behavior does not resemble very well the usual condition of the atmosphere in which strong instabilities appear always to exist.”

The above excerpt indicates the following features within the Smagorinsky model:

- Two different growth rates appeared for the first and second 30-day periods.
- An initial smaller growth rate during the first 30-day period was associated with quasi-periodic flow, but “suggested” that such a flow cannot represent the usual condition of the atmosphere. An estimated doubling time of 10 days was later reported by Lorenz (1982) [50].
- A larger growth rate, with a doubling time of six–seven days, was determined during the 2nd 30-day period, when numerical results of the Smagorinsky model displayed a more aperiodic response, indicating the early influence of Lorenz's chaos study.

The presence of two distinct growth rates signifies the existence of “two regimes” for quasi-periodic and aperiodic responses, each persisting for over 25 days. This feature is different from results obtained using the Mintz–Arakawa model. Similarly, much like the Mintz–Arakawa model, a doubling time of six–seven days indicates instability for the model equilibrium state after 259-day simulations. Such a model state could not realistically represent the atmosphere. Otherwise, a predictability of 259 days was obtained from the 259-day run.

The aforementioned features observed using the dynamical approach are summarized in Figure 2. Our analysis reaffirmed that the predictability threshold was determined based on a doubling time of five days over a 25-day period (e.g., the middle panel in Figure 2), and argued that model states following simulations exceeding 200 days (in the middle and right panels) may not reliably reflect true atmospheric conditions. Consequently, the estimated predictability limit, which served as a baseline for promoting research during the 1960s, warrants careful interpretation in light of recent advancements in modeling and prediction methodologies, as well as various metrics for predictability estimates (e.g., Table 2).

Our analysis additionally indicated that some of the features reported in Charney et al. can be found in Lorenz's theoretical models. For example, the Lorenz 1963 model displays a dependence of local growth rates on initial conditions (e.g., Shen et al., 2021a; 2022c [51,52]). Similarly, the Lorenz 1965 model suggested flow-dependent predictability, indicating the dependence of predictability limits on synoptic situations (Lorenz 1965 [53], 1984b [54]; Shen et al., 2023a [55]). The Lorenz 1969 model could produce various types of solutions, including stable, unstable, and oscillatory solutions (Shen et al., 2022a) [17]. Notably, additional findings indicated (1) that larger predictability limits (e.g., 26 or 29 days) appeared when different types of perturbations were used within the Mintz–Arakawa model, and (2) applying a doubling time (either ten days or six–seven days) within the

Smagorinsky 1963 model could lead to predictability limits exceeding two weeks, producing results consistent with that in a later study by Smagorinsky (Smagorinsky, 1969) [36]. Additional details regarding estimates of doubling times using different approaches are provided below.

2.3. Error Doubling Times Estimated Using the Empirical Approach in Lorenz (1969c) [32]

The natural occurrence of analogues (i.e., similar weather situations) was also applied for estimating growth rates during the 1960s (e.g., Lorenz 1969c) [32]. Specifically, the term “analogues” is defined as follows:

“Analogues are two states of the atmosphere that exhibit resemblance to each other. Either state in a pair of analogues can be considered equivalent to the other state plus a small superposed ‘error.’”

Thus, when two states are comparable, their differences are viewed as an error, and error growth can be estimated by observing their evolution. Such an approach, referred to as an empirical approach, was applied for estimating doubling times in Lorenz (1969c) [32]. Lorenz reported a doubling time of eight days. To overcome deficiency due to an insufficient number of observations, Lorenz applied quadratic and cubic hypotheses in order to obtain a rectified doubling time of 2.5 and 5 days, respectively (e.g., Figure 2). Please see the comments of Smagorinsky (1969) [36] below and the Supplementary Materials regarding this approach.

2.4. Major Findings within the Dynamical-Empirical Approach Using the Lorenz 1969 Model

Over the past few decades, numerous meteorology researchers have utilized key discoveries from the Lorenz 1969 model (Lorenz 1969d) [18] as a standard reference point for assessing the accuracy of model forecasts. Despite Lorenz (1993) [14] acknowledging that the two-week predictability was extrapolated from a doubling time of five days within the Mintz–Arakawa model, this particular work did not reference any of Lorenz’s 1969 studies. Moreover, up until 2006, Lorenz (1996, 2006) [23,24] maintained the perspective that the predictability problem had been partially solved. Therefore, it is crucial to determine why the meteorology community incorrectly attributes the two-week limit to numerical results derived from the Lorenz 1969 model.

To dispel misunderstandings, below, we present significant features of the 1969 model and its inherent limitations. As discussed in our recent papers (Shen et al., 2022a, 2023a [17,55]) and Lorenz’s own work (Lorenz 1984a [39]), the Lorenz 1969 model is described as a linear system with specific conditions to prevent the unbounded growth of inherently unstable solutions. This aligns with Lorenz’s description in 1984, referring to it as “a system of second-order linear ordinary differential equations.” The linear nature of the 1969 model is also recognized in Saiki and Yorke (2023) [56]. Hence, the 1969 model is not chaotic. This specific statement, along with the analysis presented in this paragraph, was shared with Prof. Tim Palmer in May 2024. Prof. Palmer has since agreed with us on this overlooked point (personal communication).

Major features of the 1969 model are summarized as follows:

- It consists of 21, linear, 2nd-order ordinary differential equations (ODEs), derived from a two-dimensional PDE that conserves vorticity.
- Coefficients for 21 ODEs were obtained based mode–mode interactions and an atmospheric kinetic energy spectrum.
- The PDE lacks baroclinic and dissipative processes and thus the 1969 model is not a turbulence model.
- While the 1969 model applied a modified quasi-normal approximation, its closure possesses inconsistent characteristics (e.g., Leith 1971 [57]) and yields unphysical outcomes (Orszag 1977 [58]; Aurell et al., 1996 [59]).
- The assumptions of “homogeneity” and “isotropy” in Lorenz (1969d) [18] do not permit variations in climatological properties from one location to another location.

- An eigenvalue analysis of the matrix for the 1969 system as well as relevant systems produces a large condition number, indicating ill-condition (Shen et al., 2022a) [17].

As a result, Shen et al. concluded that the Lorenz 1969 model is a closure-based, physically multiscale, mathematically linear, and numerically ill-conditioned system.

The above approach was referred to as the dynamical-empirical approach in the 1960s. By applying a non-uniform spectral grid, the 1969 model could examine scale interactions and predictability over a wide range of scales, from 38 m to 40,000 km (as listed in Table 3). Thus, Lorenz implicitly suggested that his model may overcome the deficiency of dynamic approaches for relatively coarse solutions that produce numerical instability or required parameterizations. As accepted by the meteorology community and as documented in Shen et al. (2022a) [17], major findings of Lorenz (1969d) [18] included the following: (1) finite predictability displays a dependence on scales; (2) smaller scale processes possess larger growth rates and smaller predictability limits; and (3) a finite time interval of reliable prediction cannot be lengthened by reducing the amplitude of initial errors. These findings can be seen in Table 3 and Figure 3. Specifically, using the 1969 model, Table 3 displays a predictability limit of 16.8 (10.1) days for a wavelength of 40,000 km (20,000 km). Here, the predictability of a specific wavelength is determined by the saturation time that is constrained by the slope of the kinetic energy spectrum. The physical meaning of the saturation and doubling times are different and, thus, predictability estimates using the two time scales should, as discussed below, be compared with caution. Additional discussions are provided in Figures S1–S3 of Supplementary Materials.

Table 3. Estimated predictability as a function of n . The first and third columns were taken from Table 3 of Lorenz (1969d) [18], while the second column for wave numbers (wavenumber $k = 1$ for the wave length $\lambda = 40,000$ km) was taken from Table 1 of Lorenz (1969d) [18]. Here, t_n indicates the saturation time for the perturbation at wavenumber $k = 2^{n-1}$.

n	k	λ	t_n
21	2^{20}	38 m	2.9 min
20	2^{19}	76	3.1
19	2^{18}	153	4.0
18	2^{17}	305	5.7
17	2^{16}	610	8.4
16	2^{15}	1221	13.0
15	2^{14}	2441	20.3
14	2^{13}	4883	32.1
13	2^{12}	9766	51.1
12	2^{11}	19,531	1.3 h
11	1024	39 km	2.2
10	512	78	3.6
9	256	156	5.8
8	128	312	9.5
7	64	625	15.7
6	32	1250	1.1 day
5	16	2500	1.8
4	8	5000	3.2
3	4	10,000	5.6
2	2	20,000	10.1
1	1	40,000	16.8

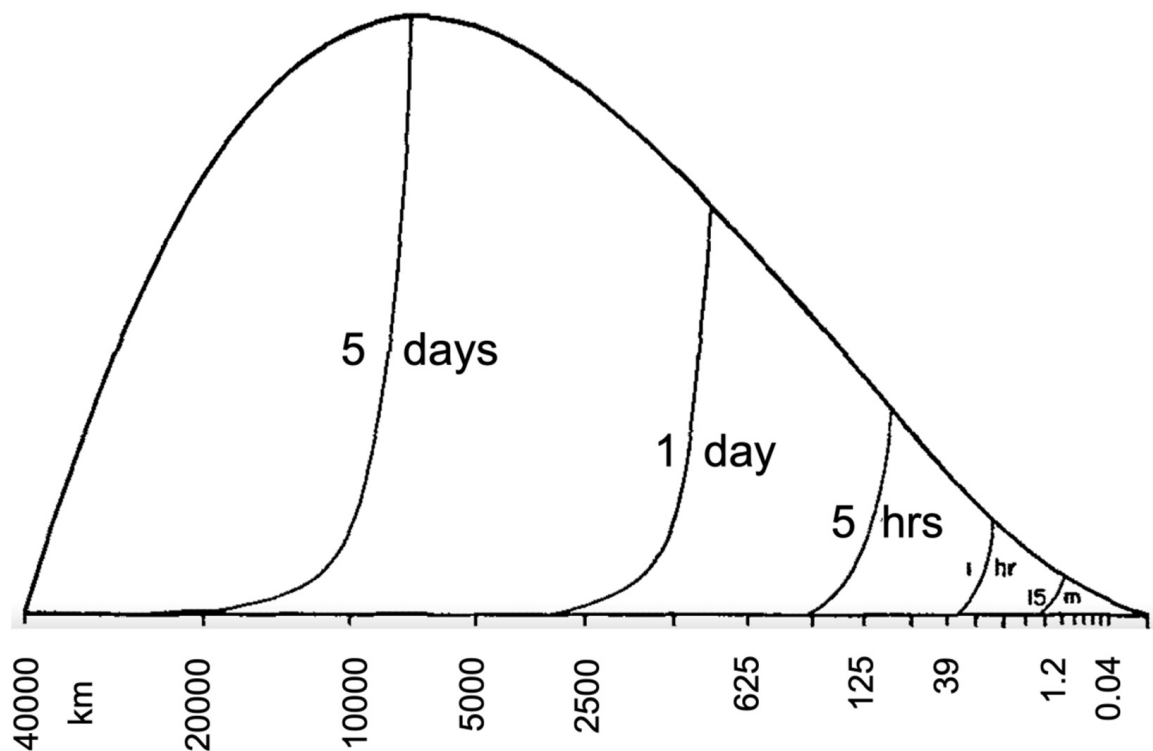


Figure 3. The dependence of estimated predictability on scales (reproduction of Figure 2 in Lorenz 1969d [18], *Tellus*).

2.5. A Revisit of the Lorenz 1969 Model and Its Relationship to a Chaotic Map

During the 1960s, an important study published as Lorenz (1969e) [33], henceforth referred to as the L69e study, greatly contributed to the dissemination of related discoveries. Published by *MIT Technology Review* in July 1969, this study, entitled “How much better can weather prediction become?”, held comparable significance to the 1969 BAMS article. The L69e study also summarized the three approaches used to determine predictability limits, including insights from the Leith, Mintz–Arakawa, and Smagorinsky models. Unlike the 1969 BAMS article that lacked any visual representations, the L69e study incorporated two figures, namely Figures 4 and 5, provided in this report. As discussed below, both figures have significant impacts, but their relationship has not been well established.

In Figure 4, Lorenz applied a difference equation, $X_{n+1} = 1.64 - X_n^2$, to illustrate the sensitive dependence of solutions on initial conditions. Such a feature was related to instability in a nonlinear system. Lorenz (1969e) [33] believed that nonlinear instability manifests within the atmosphere and can be exemplified through the nonlinear difference equation. In fact, nonlinear instability is now known as chaos since the term “chaos” was not coined until the middle of the 1970s by Li and Yorke (1975) [60]. The above difference equation is one type of quadratic map, characterized by a nonlinear quadratic term. The Logistic map, a specific type of quadratic map, is now understood to serve as a simple, yet effective, model for revealing chaos (by Lorenz 1964 [61]; Li and Yorke 1975 [60]; May 1976 [62]; Shen et al., 2023a [55]; Shen 2023, 2024 [25,63]). Stewart (2013) [64] listed the Logistic map as one of 17 equations that changed the world. The relationship between the Logistic map and the Logistic ODE is documented in Shen et al. (2023a) [55] and Shen (2024) [25].

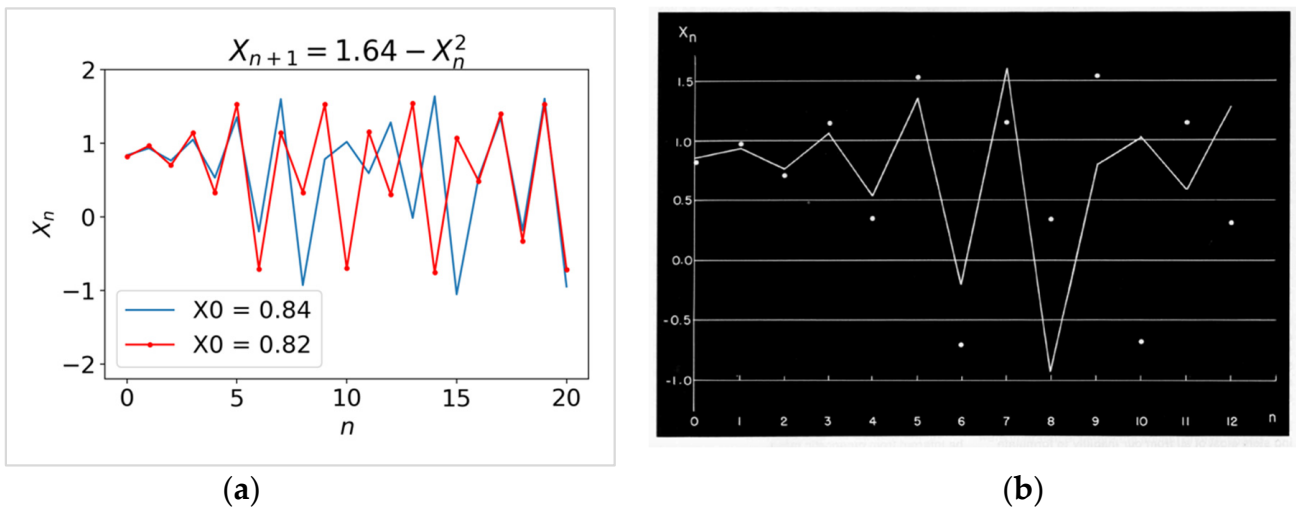


Figure 4. An illustration of the sensitive dependence of solutions on initial conditions using the difference equation, $X_{n+1} = 1.64 - X_n^2$. The left panel (a) was reproduced using a higher number of iterations. For verification, the right panel (b) was derived from Lorenz (1969e) [33].

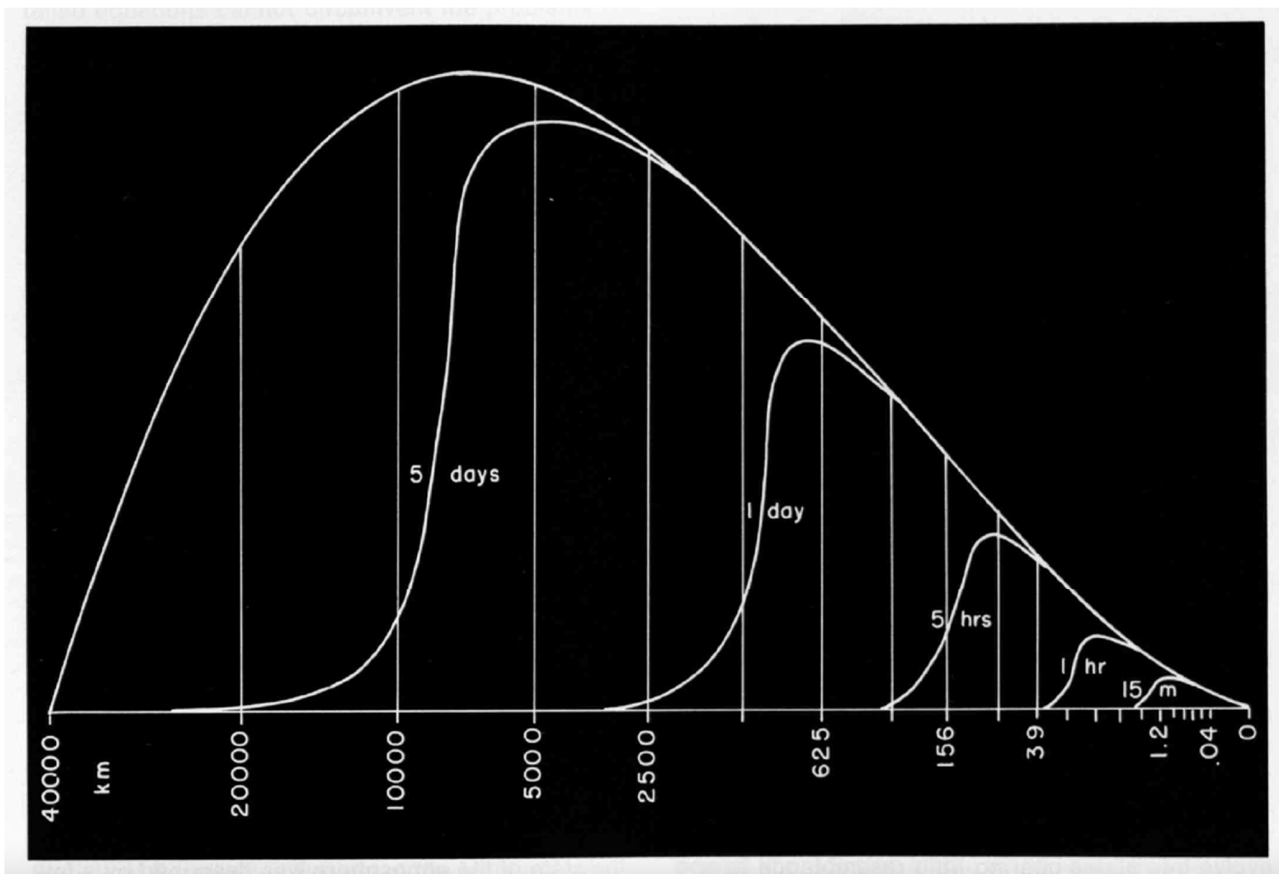


Figure 5. The dependence of the predictability limit on scales (Lorenz 1969e [33], MIT Technology Review).

Figure 5 shows the dependence of finite predictability on scales. Although Figures 4 and 5 were presented as Figures 1 and 2 in the L69e study, respectively, Lorenz did not explicitly associate the relationship between nonlinear instability in Figure 4 and finite predictability in Figure 5. A different 1969 study (i.e., the L69d study) and subsequent studies (e.g., Lorenz 1984a [39]) explicitly acknowledged that the L69 model is a linear system. Furthermore, Shen et al. (2022a) [17] suggested that finite predictability in Figure 5 is likely

associated with linear instability rather than nonlinear chaos. In fact, regarding the validity of Figure 5 (i.e., Figure 2 of the L69e) Lorenz provided the following caution:

“(Because of numerous assumptions entering the computations these results should not be regarded as the final word.)”

Other than the above, the L69e study suggested a range of predictability of approximately three weeks and, as shown below, emphasized the importance of proper interpretation of the predictability limit:

“We then conclude that the atmosphere possesses an intrinsic range of predictability of perhaps three weeks. However, if the hoped-for improvements are some day realized, still further improvements will not appreciably increase the range of predictability.

Although we feel that the evidence favoring our conclusions is substantial, we must be quick to note that they are based upon a number of assumptions which cannot be rigorously defended. We are a long way from incorporating the true atmospheric equations into our procedure. We are therefore somewhat reluctant to name a maximum range of predictability without including a safety factor.”

Based on the above excerpt and our current understanding, while the qualitative concept of finite predictability remains valid, quantitative estimates for the predictability limit should be interpreted with caution. Moreover, to date, there has not been a robust establishment of the association between predictability estimates derived from saturation times in the Lorenz 1969 linear model and a doubling time of five days in the Mintz–Arakawa model.

2.6. Impact of a Spectral Gap on Extending Predictability Horizons

In the years following 1969, to examine the impact of a spectral gap on estimates of the predictability limit, the Lorenz 1969 model was applied in four studies (Lorenz 1970, 1972, 1984a, 1985 [37–40]). A spectral gap is indicated by a separation or gap within the spectrum of kinetic energy (KE) (e.g., Figure 2 of Shen et al., 2023b [13]). The first two studies were not published, but major results in the 2nd study (i.e., Lorenz 1972 [38]) appeared in Lorenz (1985) [40]. As shown in Figure 6 (along with Figure 3 of Shen et al., 2023b [13]), results obtained without a spectral gap are comparable to those in Lorenz (1969d) [18], except that some extrapolations were applied. In contrast to the original 1969 study, the inclusion of a spectral gap in the 1972 study provided a different estimate of predictability, yielding a predictability limit of 20.6 days at a wavelength of 25,600 km, in contrast to a limit of 16.3 days without a spectral gap. Thus, if the Lorenz 1969 model with the assumption of a spectral gap can be rigorously verified, the range of predictability could be three weeks. Such a limit is quantitatively different from the findings obtained when using the original Lorenz 1969 model (e.g., Lorenz 1969d) [18] and the estimated predictability limit obtained using the Mintz–Arakawa model (Charney et al. 1966) [16].

Additionally, when using saturation time to estimate predictability horizons, raising the threshold from 90% (in Figure 6) to 95% of the saturation time can substantially extend the predictability horizons due to the asymptotic nature of the saturation time (Shen 2024) [25]. Table S1 in the Supplementary Materials outlines the progression of Lorenz’s perspectives on predictability horizons from the 1960s to 2007, as summarized in Table 1.

wave length (km)	no gap		weak gap		strong gap	
	10%	90%	10%	90%	10%	90%
12	0.8 hr	1.3 hr	1.0 hr	1.7 hr	1.0 hr	1.5 hr
25	1.3	2.1	1.8	3.1	1.8	2.9
50	2.2	3.4	3.4	6.1	3.6	7.6
100	3.5	5.6	6.1	20.7	7.8	3.5 day
200	5.8	9.2	11.1	1.4 day	2.3 day	4.6
400	9.6	15.2	0.8 day	2.0	3.7	5.5
800	15.9	1.1 day	1.4	2.7	4.7	6.3
1600	1.1 day	1.8	2.1	3.3	5.2	6.7
3200	1.9	3.1	3.0	4.3	6.0	7.6
6400	3.3	5.4	4.5	6.6	7.6	9.8
12800	5.9	9.8	7.1	11.0	10.2	14.2
25600	9.4	16.3	10.6	17.5	13.8	20.6

Figure 6. The influence of a spectral gap on estimations of predictability limits, originating from Lorenz’s unpublished work in 1972 (e.g., Lorenz 1985 [40]). Incorporating a spectral gap introduces an alternative estimate of predictability, resulting in a predictability limit of 20.6 days at a wavelength of 25,600 km. This contrasts with a limit of 16.3 days in the absence of a spectral gap. Labels “10%” and “90%” indicate times required for RMS to reach 10% and 90% of their limiting magnitudes. The numbers 16.3 and 20.6 are highlighted for the convenience of the readers.

2.7. Smagorinsky’s Comments on the Analysis of Lorenz (1969b) [31]

In 1969, Smagorinsky also published an important modeling study (Smagorinsky 1969) [36]. In this study, Smagorinsky reported high correlation coefficients of 0.7 and above for a 21-day simulation, as shown in his Figure 5 [36], and suggested the following:

“With this reservation in mind we conclude from these experiments that the deterministic limit of synoptic scale predictability is at least 3 weeks.”

Here, it is important to note that a distinct criterion, correlation coefficients, were employed to estimate predictability horizons. When evaluating predictability limits using different time scales (e.g., doubling time or saturation time) or methodologies (such as correlation coefficients or ACC), it is important to exercise caution when drawing comparisons. In contrast to the present “standard” that calculates ACC for multiple runs (e.g., Table 2), the aforementioned outcome, derived from a single run in Smagorinsky (1969) [36], may lack robustness but offers a counterexample for the two-week predictability.

Regarding the three approaches for growth rate estimates in Lorenz (1969a, b, c, d, e [18,30–33]), Smagorinsky additionally summarized the main points of Lorenz (1969b) [31], as follows:

- While the Lorenz 1969 model produced a doubling time of two–three days, the model lacked baroclinic instability.
- Within Lorenz’s analogue approach, the historical record is too short to be able to sufficiently close analogues which only differ by a measure of small error. To overcome deficiencies with large initial errors, Lorenz applied the so-called quadratic hypothesis in order to obtain a doubling time of less than three days.
- Although Mintz–Arakawa’s results reported a doubling time of five days, Lorenz’s reevaluation in 1969 (Lorenz 1969b [31], 1969e [33]) suggested a doubling time of 2.5 days.

Further discussion regarding the interpretation of a doubling time of two–three days, as well as the quadratic and cubic hypothesis, is presented in the Supplementary Materials.

3. Lorenz’s Updated Perspective and Recent Predictability Studies

The previous sections outlined how a doubling time of five days was estimated and extrapolated to establish the two-week predictability limit during the 1960s. During that time frame, Lorenz held a pessimistic perspective on the two-week predictability limit. For example, he presented various approaches estimating a doubling time of two to three days and argued against the accuracy of the Mintz–Arakawa model’s five-day doubling time. On the other hand, as reported by Reeves (2014) [15] and as reviewed by Shen et al. (2023b) [13], Lorenz’s outlook on the two-week predictability became more optimistic in the 1990s and 2000s. This shift in perspective is also evident from the fact that none of his studies from 1969 were cited when Lorenz discussed the basis for the two-week predictability limit in his book *“The Essence of Chaos,”* published in 1993.

Lorenz remained somewhat pessimistic about long-range forecasting while he spoke at the September 1981 seminar of the European Centre for Medium-Range Weather Forecasts (Lorenz 1984b) [54]. However, he also discussed potential avenues for improvement by considering the following: (1) slowly varying features, such as ocean surface temperature, sea ice, snow cover, and solar radiation; and (2) atmospheric regimes, including “blocking,” quasi-biennial oscillation, and local anomalies that show some persistence.

In 1997, Lorenz explicitly recognized the presence of extended-range predictability concerning the El Niño–Southern Oscillation (ENSO), as indicated by the following excerpt (Lorenz 1997) [65]:

“We must recognize, then, that some weather elements are predictable more than a month in advance, at least in the sense that most weather situations—even some that might well appear several years from now—are almost certain not to appear a month or two from now.

Among the most prominent features with some extended-range predictability are those associated with the El Niño–Southern Oscillation (ENSO) phenomenon.”

3.1. Recent Advances using PDE-based and AI-powered Systems

While a doubling time of 5 days was applied to determine the two-week predictability limit, as shown in Table 2, the saturation time has also been used for predictability estimates. However, saturation times longer than 2 weeks have been documented (Magnusson and Kallen 2013 [66]; Zagar and Szunyogh 2020 [67]). For instance, produced by the extended version of the Lorenz 1965 model (Lorenz 1965) [53], Figure 1 of Krishnamurthy (2019) [10] displayed a saturation time of about 100 days.

Recent studies have also reported reasonable predictions at time scales longer than two weeks (e.g., Liu et al., 2009 [68]; Shen et al., 2010 [6]; Judt 2018 [11]; Krishnamurthy 2019 [10]). For example, applying ensemble forecasts to simulate stratospheric sudden warming (Mukougawa and Hirooka 2004) [69], Mukougawa et al. (2005) [5] reported a lead time of more than two weeks. By examining the dependence of predictability on regions, Judt (2020) [12] suggested that the tropics have longer predictability than the middle latitudes and polar regions (tropics > 20 days). Using an atmosphere–ocean coupled model (or a stand-alone model), Mishra et al. (2021) [70] reported a predictability limit of 22 days (or 20 days) for Indian monsoon rainfall.

Compared to PDE-physics-based methods, machine learning (ML), or more broadly, artificial intelligence (AI) methods have shown promise in improving weather predictions (Weyn et al., 2019, 2020, 2021 [71–73]; Rasp and Thuerey 2021 [74]; Pathak et al., 2022 [75]; Bi et al., 2023 [76]; Bonev et al., 2023 [77]; Chen, Han, et al., 2023 [78]; Chen, Zhong et al., 2023 [79]; Nguyen. et al., 2023 [80]; Lam et al., 2023 [81]; Selz and Craig 2023 [82]; Watt-Meyer et al., 2023 [83]; Bach et al., 2024 [84]; Bouallègue et al., 2024 [85]; Li et al., 2024 [86]). As shown in Table 4, these AI-powered models were trained using the ERA5 reanalysis dataset (Hersbach et al., 2018, 2020) [87,88] and CMIP6 data (Eyring et al., 2016 [89]) and assessed using various metrics including RMSE, ACC, Contin-

uous Ranked Probability Score (CRPS), Temporal Anomaly Correlation Coefficient (TCC), Ranked Probability Skill Score (RPSS), Brier Skill Score (BSS), and bivariate correlation (COR).

Table 4. A list of major AI-powered systems.

Study	Model's Name	AI Technology	Data	Simulation Length	Evaluation Metric	Remark
Weyn et al. (2020) [72]	Deep Learning Weather Prediction (DLWP)	CNN	ERA5, 1979–2018, 2°	up to 7 days	RMSE, ACC	
Weyn et al. (2021) [73]		CNN	ERA5, 1979–2018, 1.4°	up to 6 weeks	RMSE, ACC, Continuous Ranked Probability Score (CRPS)	
Rasp and Thuerey (2021) [74]	WeatherBench ResNet	Residual Neural Network (ResNet)	ERA5, 1979–2018; CMIP6, climate model simulations	up to 5 days	RMSE, ACC	
Bi et al. (2023) [76]	Pangu-Weather	(modified) Vision Transformer	ERA5, 1979–2017, 2.5°	up to 7 days	RMSE, ACC	
Selz and Craig (2023) [82]	the same	the same	the same	up to 72 h	RMSE, ACC	study butterfly effect
Bouallègue et al. (2024) [85]	the same	the same	the same	up to 10 days	the same	in an operational-like context
Lam et al. (2023) [81]	GraphCast	Graph Neural Network (GNN)	ERA5, 1979–2018, 2.5°	up to 14 days	RMSE, ACC	developed by Google
Pathak et al. (2022); Bonev et al. (2023) [75,77]	FourCast Net	Vision Transformer with Fourier Neural Operators	ERA5, 1979–2018, 2.5°	up to 1 or 2 weeks	ACC	manuscript posted; sponsored by Nvidia
Watt-Meyer et al. (2023) [83]	ACE	the same	the same FVGFS	10 years	RMSE, time-mean RMSE	ACE stands for AI2 Climate Emulator
Nguyen et al. (2023) [80]	CimaX	Vision Transformer	CMIP6, 1850–current, various; ERA5, 1979–2018, 2.5°	up to 1 month	RMSE, ACC	sponsored by Microsoft
Chen, Zhong, et al. (2023) [79]	FuXi	modified Vision Transformer	ERA5, 1979–2018, 2.5°	up to 15 days	RMSE, ACC, CRPS	
Li et al. (2024) [86]	FuXi-S2S	Enhanced FuXi base model with other modules	ERA5, 1950–2021, 1.5°	up to 42 days	TCC, RPSS, BSS, COR	manuscript posted 14 February 2024
Chen, Han, et al. (2023) [78]	FengWu	a cross-modal fusion transformer	ERA5, 1979–2018, 2.5°	up to 14 days	RMSE, ACC	
Bach et al. (2024) [84]	hybrid dynamical and data-driven methods	EOF, Neural network architecture, Ensemble Oscillation Correction (EnOC)	ERA5, 1979–2018, 2.5°; IMD rainfall, 1901–2016	up to 46 days	RMSE, ACC, Bivariate Correlation Coefficient	

As summarized in Table 4, by applying deep convolutional neural networks (CNNs), Weyn et al. (2019) [71] reported lead times of 14 days. More importantly, recent advances in AI technology, particularly transformer technology (e.g., Vaswani et al., 2017) [90] and its variants, including the “vision transformer” (Dosovitskiy et al., 2020 [91]), have offered significant opportunities to reduce the cost of weather predictions and revisit the predictability limit. Table 4 lists major AI-powered systems, most of which were published in 2023 and 2024 following the widespread recognition of transformer technology due to its major application in ChatGPT. Among the listed AI-powered systems, as compared to PDE-physics-based systems, all produced comparable or slightly better predictions for conventional short-term forecasts (3–14 days). Three studies have attempted to perform simulations at subseasonal or larger scales. Among the three studies, the ClimX system

was reported in a conference article. The enhanced Fu-Xi system (and its base version) was documented in a preprint article (and journal article). In the 3rd study, the hybrid dynamical and data-driven approach was applied by Bach et al. (2024, PNAS) [84] to successively demonstrate the potential for improving subseasonal monsoon prediction. As derived from their study, Figure 7 displays a correlation above 0.5 over a 46-day period in two predictions. While correlation coefficients (as depicted in Figure 7) or Anomaly Correlation Coefficients (ACC) have recently been utilized to assess predictability horizons, the concept of doubling time, illustrated in the Supplementary Materials, was employed in the 1960s to estimate a two-week predictability limit.

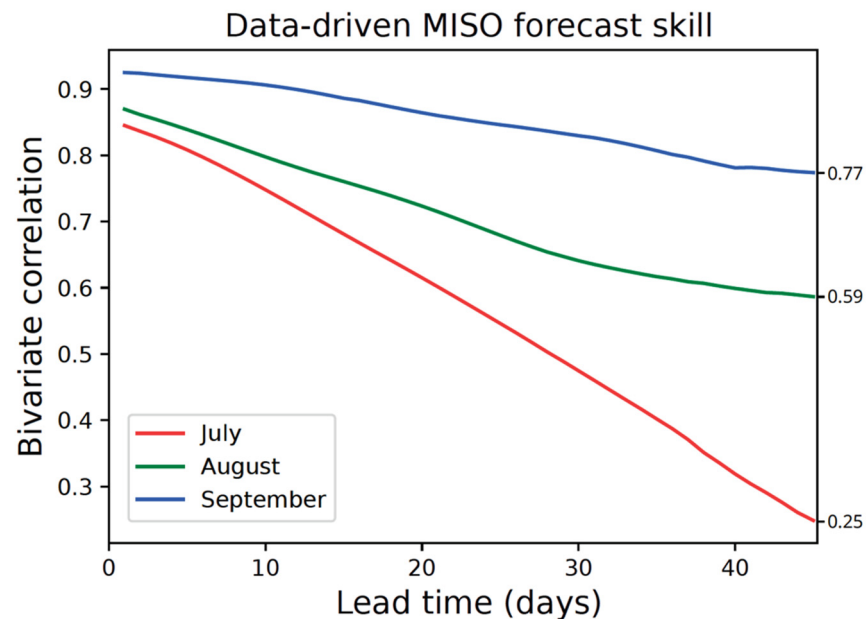


Figure 7. Time-varying correlation coefficient between predicted and observed monsoon intraseasonal oscillation (MISO) modes, for forecasts initiated on the 1st of July, August, and September, spanning the years 2008 to 2016. (Bach et al. (2024) [84]).

After submitting our manuscript in late May 2024, we discovered several additional studies employing AI-powered systems. These include, but are not limited to, works by Bodnar et al. (2024) [92], Kochhov et al. (2024) [93], Lang et al. (2024) [94], Mardani et al. (2023) [95], Price et al. (2024) [96], Vonich and Hakim (2024) [97], and Wu and Xue (2024) [98], all demonstrating the swift advancements facilitated by AI. Notably, Wu and Xue (2024) [98] conducted a thorough review of AI-based models from a developmental viewpoint. Lang et al. (2024) [94] described the ECMWF's AI-based system. Kochhov et al. (2024) [93] introduced a novel model that integrates PDEs and ML to generate ensemble weather forecasts more accurately, as assessed by CRPS, than the existing ECMWF model. Vonich and Hakim (2024) [97] reported a predictability of 23 days for the Pacific Northwest heatwave.

Although the above systems have not yet established a new predictability horizon, our suggestion in Table 1, viewing the two-week limit as a predictability hypothesis, makes it easier for scientists to understand why the above promising results with specific weather systems are possible and encourage attempts for proving or disproving the predictability hypothesis. More importantly, AI-powered methods provide alternative, cost-effective approaches.

3.2. A View of Distinct Predictability Using a Generalized Lorenz Model

By guiding the choice of numerical results from real-world models, the concept of Lorenz's chaos, characterized by aperiodic features and instability, indeed, indirectly influenced the establishment of the two-week predictability limit. Specifically, the key

characteristics of Lorenz's 1963 and 1969 models provide evidence for the existence of a predictability limit. However, it is important to note that the underlying mechanisms or sensitivities that lead to finite predictability differ between these models (e.g., as discussed in Shen et al., 2021a [51], 2022a, c [17,52]).

Lorenz's 1963 model is characterized by its limited scale and chaotic nature, while the Lorenz 1969 model is closure-based, physically multiscale, mathematically linear, and numerically ill-conditioned. Furthermore, as elaborated on in Section 3.1.2 of Shen et al., 2022a [17], the Lorenz 1969 ill-conditioned system tends to easily capture numerical instability.

As discussed by Shen et al. (2023a) [55] and Shen (2023a) [63], most of Lorenz's models did not incorporate spatial and time-varying "backgrounds." For example, the Lorenz 1963 model utilized time-independent parameters and the Lorenz 1969 model applied a time-independent kinetic energy spectrum, as well as assumed homogeneity and isotropy. To address this limitation, we employed a generalized Lorenz model (Shen 2019a [99]; Shen et al., 2019 [100]) and applied a time-varying parameter that emulates the impact of slowly varying variables.

As illustrated by Shen et al. (2021a) [51], the Rayleigh parameter is set to a periodic function of time that allows different types of solutions; equations for the generalized Lorenz model are additionally provided in the Supplementary Materials of Shen et al. (2021a) [51]. Our findings revealed the coexistence of chaotic and non-chaotic properties, including nonlinear oscillations (i.e., limit cycle solutions), and the coexistence of rapidly and slowly varying solutions (Shen et al., 2021a) [51]. Such findings challenge the conventional view that the system is solely chaotic and suggest a revised view on the dual nature of chaos and order with coexisting short-term and long-term predictability. For example, the appearance of the theoretical nonlinear oscillations could provide a support to the existence of oscillations such as monsoon intraseasonal oscillation (MISO) for better predictability, as discussed above in Figure 7 (Bach et al., 2004) [84]. The concept of attractor coexistence also helped us uncover regional dependencies, such as blocking patterns and seasonal variations.

Furthermore, as depicted in Figure 5 of Shen et al. (2022c) [52], our generalized Lorenz model results suggest the possibility of regime transitions between regular and chaotic solutions. Both the previously mentioned studies and recent research (e.g., Zeng 2023) [101] support Lorenz's 1997 updated perspective, suggesting a possibility for the coexisting long predictability of ENSO and short-term predictability (i.e., 2-week predictability, when applicable).

3.3. Proposed Future Research Directions

The "Next Generation Earth System Prediction: Strategies for Subseasonal to Seasonal Forecasts" report by the National Academy of Sciences (2016) [3] underscores the societal benefits of the broad implementation of subseasonal to seasonal (S2S) forecasts, which provide predictions ranging from two weeks to twelve months ahead. The report projects that S2S forecasts will become as commonplace as daily weather reports, playing a vital role in sectors such as agriculture, water management, and public health. These forecasts are pivotal in reducing risks associated with extreme weather events, thereby safeguarding lives and reducing economic losses. The report points out a significant disparity in the support for S2S forecasts compared to immediate weather predictions and long-term climate projections, and it identifies substantial challenges, including the need for forecasts that align more closely with the specific temporal and spatial requirements of users. It calls for collaborative efforts between physical and social scientists to enhance the applicability of S2S forecasts across various decision-making scenarios. Concurrently, as mentioned in Section 3.2, recent advancements in AI and ML have produced promising forecasts that extend beyond two weeks (refer to Figure 7) and have improved forecast customization through techniques such as downscaling, as demonstrated by Mardani et al. (2023) [95], highlighting the critical role of data scientists in this field.

Building on the insights from this report and previous research, we are optimistic that ongoing innovations in both practical and theoretical modeling, augmented by artificial

intelligence, will continually enhance our understanding and prediction of weather phenomena. These advancements are especially beneficial for investigating pivotal phenomena such as the butterfly effect (model sensitivities), multiscale interactions, and multistability, which encompass feedback from numerically or physically small-scale processes, modulation by large-scale systems, and predictability that varies with different types of weather systems. To advance these efforts, we propose a series of research areas that would benefit from an integrated approach combining PDE-based methods and AI-enhanced techniques:

1. Enhancing numerical methods by implementing variable time steps.
2. Fusing AI with ensemble forecasting to refine predictive accuracy.
3. Measuring the sensitivity dependence on initial conditions (SDIC)—i.e. the butterfly effect—and chaotic behaviors in AI-driven systems.
4. Improving spatial and/or temporal resolution through AI-powered downscaling.
5. Expanding the functionality of AI models by integrating non-forecast variables.
6. Discovering multiscale processes via singular value analysis of query, key, and value matrices.
7. Crafting conceptual models to deepen the understanding of predictability.
8. Reevaluating the boundaries of predictability horizons.
9. Evaluating how the temporal extent of reanalysis data affects the precision of climate projections.
10. Investigating AI-based model hallucinations and their linkage to sensitive dependence on initial conditions.

For additional details, please refer to Shen et al. (2024) [102].

4. Concluding Remarks

This study, along with our recent research (e.g., Table 1), suggests that the widely recognized two-week predictability limit was initially estimated based on a five-day doubling time using a general circulation model, rather than being a direct outcome of Lorenz's chaotic models. To provide a clearer perspective on the two-week predictability limit, we propose the following statement:

“Much like Moore’s Law in the realm of computing, the predictability limit hypothesis, specifically the two-week predictability limit, is an empirical association based on practical modeling and idealized chaotic modeling from the 1960s. It stands as a limited set of observed findings and as a reasonable extrapolation from early modeling results during the 1960s, rather than constituting fundamental physics.”

The Predictability Limit Hypothesis in Table 1 summarizes the historical context of predictability research, encompassing real-world, theoretical models, and other approaches from the 1960s. Our reevaluation highlights quantitative estimates of two-week predictability using the Mintz–Arakawa model, as well as qualitative, finite predictability within Lorenz’s 1963 and 1969 models, under the leadership of Charney et al. This concept also aligns with Lorenz’s evolved perspective on predictability limits in the 1990s and 2000s. Since the two-week predictability limit was derived from a five-day doubling time, the notion of continuous improvement in predictability horizons by reducing initial errors suggests that this limit should not be viewed as a rigid upper boundary.

Furthermore, our revisit indicates that doubling times depend on a model’s long-term states and different approaches. Our analysis also suggest larger predictability limits reported in the 1960s and 1970s, including 26 and 29 days when various perturbations were introduced and 20.6 days when a kinetic energy spectral gap was included within the Lorenz 1969 model.

Our studies, combined with our previous research (e.g., Shen et al., 2021a; 2022c [51,52]), highlight cumulative advancements in both PDE-physics-based and AI-powered systems since the 1960s, which have shown promising results in long-term simulations. Although these simulations extend beyond the traditional two-week limit, they do not contradict the Predictability Limit Hypothesis based on 1960s models. This new concept helps explain

why the practical capabilities of current models are still consistent with the major findings of finite predictability within Lorenz's theoretical models.

Recognizing that weather prediction is a combined boundary-initial value problem imposes constraints on temporal changes. This concept can also extend to examine the predictability of seasonal, yearly, decadal, and longer climate predictions. The feasibility of this approach was illustrated by developing a unified weather and climate model, which led to successful short-term weather predictions in the early 2000s (e.g., Lin et al., 2003 [22]; Atlas et al., 2005 [103]; Shen et al., 2006a [104], 2006b [105], 2010 [6], 2011 [7]). In comparison, AI-powered systems trained over several decades using ERA5 reanalysis and/or CMIP6 data can be viewed as weather-climate unified systems. Both weather and climate forecasts predict changes in the state of variables such as temperature and precipitation, then compute their averages over different time scales. With weather, this can involve hourly or daily averages, while climate focuses on yearly and longer-term statistics. Both forecasts essentially use the same mathematical framework (with climate involving more nonlinear interactions) within PDE-physics-based or AI-powered systems. The question remains whether and how the concepts discussed for short time scales can extend to climate prediction at longer time scales.

Supplementary Materials: The following supporting information can be downloaded at: <https://www.mdpi.com/article/10.3390/atmos15070837/s1>, Table S1 illustrates the evolution of Lorenz's perspectives on predictability horizons since the 1960s. Figure S1 depicts predictability estimates based on doubling time (Paxson and Shen 2022 [106]). Figure S2 displays RMS errors, indicating a doubling time of 2.9 days and a saturation time of 100 days (Krishnamurthy 2019 [10]). Figure S3 demonstrates the dependence of error growth rates on geographical locations (Reynolds et al. 1994 [107]; Kalnay 2002 [108]). This idea is further connected to the concept of coexisting attractors with distinct predictability (e.g., Shen et al., 2021b [109]) in the Supplementary Materials.

Author Contributions: B.-W.S. designed and performed research; B.-W.S., R.A.P.S., X.Z. (Xubin Zeng) and X.Z. (Xiping Zeng) wrote the paper. All authors have read and agreed to the published version of the manuscript.

Funding: This research received no external funding.

Acknowledgments: We thank anonymous reviewers, academic editors, and editors for valuable comments and discussions.

Conflicts of Interest: The authors declare no conflict of interest.

References

1. National Academies of Sciences, Engineering, and Medicine. *Earth System Predictability Research and Development: Proceedings of a Workshop in Brief*; The National Academies Press: Washington, DC, USA, 2020. [CrossRef]
2. National Research Council. *When Weather Matters: Science and Services to Meet Critical Societal Needs*; The National Academies Press: Washington, DC, USA, 2010. [CrossRef]
3. National Academies of Sciences, Engineering, and Medicine. *Next Generation Earth System Prediction: Strategies for Subseasonal to Seasonal Forecasts*; The National Academies Press: Washington, DC, USA, 2016. [CrossRef]
4. Sonechkin, D.M.; Samrov, V.P.; Zimin, N.E. The Model Averaged with Respect to Planetary Wave Phases Reveals the Ability to Overcome the Weekly Predictability Limit. *Mon. Weather Rev.* **1995**, *123*, 2461–2473. [CrossRef]
5. Mukougawa, H.; Sakai, H.; Hirooka, T. High Sensitivity to the Initial Condition for the Prediction of Stratospheric Sudden Warming. *Geophys. Res. Lett.* **2005**, *32*, L17806. [CrossRef]
6. Shen, B.-W.; Tao, W.-K.; Wu, M.-L. African Easterly Waves in 30-day High-resolution Global Simulations: A Case Study during the 2006 NAMMA Period. *Geophys. Res. Lett.* **2010**, *37*, L18803. [CrossRef]
7. Shen, B.-W.; Tao, W.-K.; Green, B. Coupling Advanced Modeling and Visualization to Improve High-Impact Tropical Weather Prediction (CAMVis). *IEEE Comput. Sci. Eng. (CiSE)* **2011**, *13*, 56–67. [CrossRef]
8. Shen, B.-W. On the Predictability of 30-day Global Mesoscale Simulations of Multiple African Easterly Waves during Summer 2006: A View with a Generalized Lorenz Model. *Geosciences* **2019**, *9*, 281. [CrossRef]
9. Krishnamurthy, V.; Sharma, A. Predictability at intraseasonal time scale. *Geophys. Res. Lett.* **2017**, *44*, 8530–8537. [CrossRef]
10. Krishnamurthy, V. Predictability of weather and climate. *Earth Space Sci.* **2019**, *6*, 1043–1056. [CrossRef] [PubMed]
11. Judt, F. Insights into Atmospheric Predictability through Global Convection-Permitting Model Simulations. *J. Atmos. Sci.* **2018**, *75*, 1477–1497. [CrossRef]

12. Judt, F. Atmospheric predictability of the tropics, middle latitudes, and polar regions explored through global storm-resolving simulations. *J. Atmos. Sci.* **2020**, *77*, 257–276. [[CrossRef](#)]
13. Shen, B.-W.; Pielke, R.A., Sr.; Zeng, X.; Zeng, X. 2023b: Lorenz's View on the Predictability Limit. *Encyclopedia* **2023**, *3*, 887–899. [[CrossRef](#)]
14. Lorenz, E.N. *The Essence of Chaos*; University of Washington Press: Seattle, WA, USA, 1993; 227p.
15. Reeves, R.W. Edward Lorenz Revisiting the Limits of Predictability and Their Implications: An Interview from 2007. *Bull. Am. Meteorol. Soc.* **2014**, *95*, 681–687. [[CrossRef](#)]
16. Charney, J.G.; Fleagle, R.G.; Lally, V.E.; Riehl, H.; Wark, D.Q. The feasibility of a global observation and analysis experiment. *Bull. Am. Meteorol. Soc.* **1966**, *47*, 200–220.
17. Shen, B.-W.; Pielke, R.A., Sr.; Zeng, X. One Saddle Point and Two Types of Sensitivities within the Lorenz 1963 and 1969 Models. *Atmosphere* **2022**, *13*, 753. [[CrossRef](#)]
18. Lorenz, E.N. The predictability of a flow which possesses many scales of motion. *Tellus* **1969**, *21*, 19.
19. Vallis, G. *Atmospheric and Oceanic Fluid Dynamics*; Cambridge University Press: Cambridge, UK, 2006; 745p.
20. Lloveras, D.J.; Tierney, L.H.; Durran, D. Mesoscale Predictability in Moist Midlatitude Cyclones Is Not Sensitive to the Slope of the Background Kinetic Energy Spectrum. *J. Atmos. Sci.* **2022**, *79*, 119–139. [[CrossRef](#)]
21. Owens, R.G.; Hewson, T.D. *ECMWF Forecast User Guide*; ECMWF: Reading, UK, 2018. [[CrossRef](#)]
22. Lin, S.-J.; Shen, B.-W.; Putman, W.P.; Chern, J.-D. Application of the high-resolution finite-volume NASA/NCAR Climate Model for Medium-Range Weather Prediction Experiments. In Proceedings of the EGS-AGU-EUG Joint Assembly, Nice, France, 6–11 April 2003.
23. Lorenz, E.N. Predictability—A problem partly solved. In Proceedings of the Seminar on Predictability, Reading, UK, 4–8 September 1995; ECMWF: Reading, UK, 1996; Volume 1.
24. Lorenz, E.N. Predictability—A problem partly solved. In *Predictability of Weather and Climate*; Palmer, T., Hagedorn, R., Eds.; Cambridge University Press: Cambridge, UK, 2006; pp. 40–58.
25. Shen, B.-W. Revisiting Lorenz's Error Growth Models: Insights and Application. *Encyclopedia* **2024**. [[CrossRef](#)]
26. Pegion, K.; DelSole, T.; Becker, E.; Cicerone, T. 2019: Assessing the fidelity of predictability estimates. *Clim. Dyn.* **2019**, *53*, 7251–7265. [[CrossRef](#)]
27. Lorenz, E.N. Deterministic nonperiodic flow. *J. Atmos. Sci.* **1963**, *20*, 130–141. [[CrossRef](#)]
28. Gleick, J. *Chaos: Making a New Science*; Penguin: New York, NY, USA, 1987; 360p.
29. Stewart, I. *Does God Play Dice?* Blackwell Publishing Ltd.: Hoboken, NJ, USA, 1989; 401p.
30. Lorenz, E.N. *Studies of Atmospheric Predictability. [Part 1] [Part 2] [Part 3] [Part 4] Final Report, February, Statistical Forecasting Project*; Air Force Research Laboratories, Office of Aerospace Research, USAF: Bedford, MA, USA, 1969; 145p.
31. Lorenz, E.N. Three approaches to atmospheric predictability. *Bull. Am. Meteorol. Soc.* **1969**, *50*, 345–351.
32. Lorenz, E.N. Atmospheric predictability as revealed by naturally occurring analogues. *J. Atmos. Sci.* **1969**, *26*, 636–646. [[CrossRef](#)]
33. Lorenz, E.N. How much better can weather prediction become? *MIT Technol. Rev.* **1969**, 39–49.
34. Lorenz, E.N. The nature of the global circulation of the atmosphere: A present view. *The Global Circulation of the Atmosphere*, London, Roy. Meteor. Soc. **1969**, 3–23.
35. GARP. GARP topics. *Bull. Am. Meteorol. Soc.* **1969**, *50*, 136–141.
36. Smagorinsky, J. Problems and promises of deterministic extended range forecasting. *Bull. Am. Meteorol. Soc.* **1969**, *50*, 286–312. [[CrossRef](#)]
37. Lorenz, E.N. Progress Report on Atmospheric Predictability. Never Printed. 1970.
38. Lorenz, E. Limits of Meteorological Predictability. Prepared for the American Meteorological Society, February. Unpublished. 1972.
39. Lorenz, E.N. Estimates of atmospheric predictability at medium range. In *Predictability of Fluid Motions*; Holloway, G., West, B., Eds.; American Institute of Physics: New York, NY, USA, 1984; pp. 133–139.
40. Lorenz, E.N. The growth of errors in prediction. In *Turbulence and Predictability in Geophysical Fluid Dynamics and Climate Dynamics*; Società Italiana di Fisica: Bologna, Italy, 1985; pp. 243–265.
41. Rotunno, R.; Snyder, C. A generalization of Lorenz's model for the predictability of flows with many scales of motion. *J. Atmos. Sci.* **2008**, *65*, 1063–1076. [[CrossRef](#)]
42. Durran, D.R.; Gingrich, M. 2014: Atmospheric predictability: Why atmospheric butterflies are not of practical importance. *J. Atmos. Sci.* **2014**, *71*, 2476–2478. [[CrossRef](#)]
43. Palmer, T.N.; Doring, A.; Seregin, G. The real butterfly effect. *Nonlinearity* **2014**, *27*, R123–R141. [[CrossRef](#)]
44. Sun, Y.Q.; Zhang, F. A New Theoretical Framework for Understanding Multiscale Atmospheric Predictability. *J. Atmos. Sci.* **2020**. [[CrossRef](#)]
45. Shen, B.-W.; Pielke, R.A., Sr.; Zeng, X.; Cui, J.; Faghih-Naini, S.; Paxson, W.; Atlas, R. Three Kinds of Butterfly Effects Within Lorenz Models. *Encyclopedia* **2022**, *2*, 1250–1259. [[CrossRef](#)]
46. Leith, C.E. *Numerical Simulation of the Earth's Atmosphere. Methods in Computational Physics*; Academic Press: New York, NY, USA, 1965; Volume 4, pp. 1–28.
47. Mintz, Y. Very long-term global integration of the primitive equations of atmospheric motion. In *WMO-IUGG Symposium on Research and Development Aspects of Long-Range Forecasting*; Tech. Note No. 66; World Meteorological Organization: Geneva, Switzerland, 1964; pp. 141–155.

48. Smagorinsky, J. General circulation experiments with the primitive equations. I. The basic experiment. *Mon. Weather Rev.* **1963**, *91*, 99–164. [[CrossRef](#)]
49. Lewis, J. Roots of ensemble forecasting. *Mon. Weather. Rev.* **2005**, *133*, 1865–1885. [[CrossRef](#)]
50. Lorenz, E.N. Atmospheric predictability experiments with a large numerical model. *Tellus* **1982**, *34*, 505–513. [[CrossRef](#)]
51. Shen, B.-W.; Pielke Sr., R.A.; Zeng, X.; Baik, J.-J.; Faghih-Naini, S.; Cui, J.; Atlas, R. Is Weather Chaotic? Coexistence of Chaos and Order within a Generalized Lorenz Model. *Bull. Am. Meteorol. Soc.* **2021**, *2*, E148–E158. [[CrossRef](#)]
52. Shen, B.-W.; Pielke Sr., R.A.; Zeng, X.; Cui, J.; Faghih-Naini, S.; Paxson, W.; Kesarkar, A.; Zeng, X.; Atlas, R. The Dual Nature of Chaos and Order in the Atmosphere. *Atmosphere* **2022**, *13*, 1892. [[CrossRef](#)]
53. Lorenz, E.N. A study of the predictability of a 28-variable atmospheric model. *Tellu* **1965**, *17*, 321–333. [[CrossRef](#)]
54. Lorenz, E.N. Some aspects of atmospheric predictability. European Centre for Medium Range Weather Forecasts, Seminar 1981. In Proceedings of the Problems and Prospects in Long and Medium Range Weather Forecasting, Reading, UK, 14–18 September 1984; pp. 1–20, (BWS: This study was presented in 1981 and cited as 1982 by Lorenz in his web site. However, it was published in 1984.).
55. Shen, B.-W.; Pielke, R.A., Sr.; Zeng, X. 50th Anniversary of the Metaphorical Butterfly Effect since Lorenz (1972): Special Issue on Multistability, Multiscale Predictability, and Sensitivity in Numerical Models. *Atmosphere* **2023**, *14*, 1279. [[CrossRef](#)]
56. Saiki, Y.; Yorke, J.A. Can the Flap of a Butterfly’s Wings Shift a Tornado into Texas—Without Chaos? *Atmosphere* **2023**, *14*, 821. [[CrossRef](#)]
57. Leith, C.E. Atmospheric predictability and two-dimensional turbulence. *J. Atmos. Sci.* **1971**, *28*, 145–161. [[CrossRef](#)]
58. Orszag, S.A. *Fluid Dynamics*; Balian, R., Peube, J.L., Eds.; Gordon and Breach: London, UK, 1977.
59. Aurell, E.; Boffetta, G.; Crisanti, A.; Paladin, G.; Vulpiani, A. Predictability in systems with many characteristic times: The case of turbulence. *Phys. Rev. E* **1996**, *53*, 2337–2349. [[CrossRef](#)]
60. Li, T.Y.; Yorke, J.A. Period Three Implies Chaos. *Am. Math. Mon.* **1975**, *82*, 985–992. [[CrossRef](#)]
61. Lorenz, E.N. The problem of deducing the climate from the governing equations. *Tellus* **1964**, *16*, 1–11. [[CrossRef](#)]
62. May, R.M. Simple mathematical models with very complicated dynamics. *Nature* **1976**, *261*, 459–467. [[CrossRef](#)] [[PubMed](#)]
63. Shen, B.-W. A Review of Lorenz’s Models from 1960 to 2008. *Int. J. Bifurc. Chaos* **2023**, *33*, 2330024. [[CrossRef](#)]
64. Stewart, I. *Seventeen Equations That Changed the World*; Profile Book: London, UK, 2013; 342p.
65. Lorenz, E.N. Climate is what you expect. [Prepared for publication by NCAR; unknown if actually printed. Possibly related to presentation at NCAR colloquium, Applications of statistics to modeling the Earth’s climate system, November 1994]. 1997.
66. Magnusson, L.; Källén, E. Factors Influencing Skill Improvements in the ECMWF Forecasting System. *Mon. Weather. Rev.* **2013**, *141*, 3142–3153. [[CrossRef](#)]
67. Zagar, N.; Szunyogh, I. Comments on “What Is the Predictability Limit of Midlatitude Weather?”. *J. Atmospheric Sci.* **2020**, *77*, 781–785. [[CrossRef](#)]
68. Liu, H.-L.; Sassi, F.; Garcia, R.R. Error Growth in a Whole Atmosphere Climate Model. *J. Atmos. Sci.* **2009**, *66*, 173–186. [[CrossRef](#)]
69. Mukougawa, H.; Hirooka, T. Predictability of stratospheric sudden warming: A case study for 1998/99 winter. *Mon. Weather Rev.* **2004**, *132*, 1764–1776. [[CrossRef](#)]
70. Mishra, A.K.; Dwivedi, S.; Di Sante, F. Performance of the RegCM-MITgcm Coupled Regional Model in Simulating the Indian Summer Monsoon Rainfall. *Pure Appl. Geophys.* **2021**, *178*, 603–617. [[CrossRef](#)]
71. Weyn, J.A.; Durran, D.R.; Caruana, R. Can Machines Learn to Predict Weather? Using Deep Learning to Predict Gridded 500-hPa Geopotential Height from Historical Weather Data. *J. Adv. Model. Earth Syst.* **2019**, *11*, 2680–2693. [[CrossRef](#)]
72. Weyn, J.A.; Durran, D.R.; Caruana, R. Improving data-driven global weather prediction using deep convolutional neural networks on a cubed sphere. *J. Adv. Model. Earth Syst.* **2020**, *12*, e2020MS002109. [[CrossRef](#)]
73. Weyn, J.; Durran, D.; Caruana, R.; Cresswell-Clay, N. Sub-seasonal forecasting with a large ensemble of deeplearning weather prediction models. *J. Adv. Model. Earth Syst.* **2021**, *13*, e2021MS002502. [[CrossRef](#)]
74. Rasp, S.; Thuerey, N. Data-driven medium-range weather prediction with a Resnet pretrained on climate simulations: A new model for WeatherBench. *J. Adv. Model. Earth Syst.* **2021**, *13*, e2020MS002405. [[CrossRef](#)]
75. Pathak, J.; Subramanian, S.; Harrington, P.; Raja, S.; Chattopadhyay, A.; Mardani, M.; Kurth, T.; Hall, D.; Li, Z.; Aizzadenesheli, K.; et al. Fourcastnet: A Global Data-Driven High-Resolution Weather Model Using Adaptive Fourier Neural Operators. *arXiv* **2022**, arXiv:2202.11214.
76. Bi, K.; Xie, L.; Zhang, H.; Chen, X.; Gu, X.; Tian, Q. Accurate medium-range global weather forecasting with 3D neural networks. *Nature* **2023**, *619*, 533–538. [[CrossRef](#)]
77. Bonev, B.; Kurth, T.; Hundt, C.; Pathak, J.; Baust, M.; Kashinath, K.; Anandkumar, A. Spherical Fourier Neural Operators: Learning Stable Dynamics on the Sphere. *arXiv* **2023**, arXiv:2306.03838.
78. Chen, K.; Han, T.; Gong, J.; Bai, L.; Ling, F.; Luo, J.J.; Chen, X.; Ma, L.; Zhang, T.; Su, R.; et al. FengWu: Pushing The Skillful Global Medium-Range Weather Forecast Beyond 10 Days Lead. *arXiv* **2023**, arXiv:2304.02948.
79. Chen, L.; Zhong, X.; Zhang, F.; Cheng, Y.; Xu, Y.; Qi, Y.; Li, H. FuXi: A cascade machine learning forecasting system for 15-day global weather forecast. *NPJ Clim. Atmos. Sci.* **2023**, *6*, 190. [[CrossRef](#)]
80. Nguyen, T.; Brandstetter, J.; Kapoor, A.; Gupta, J.K.; Grover, A. Climax: A Foundation Model for Weather and Climate. *arXiv* **2023**, arXiv:2301.10343.

81. Lam, R.; Sanchez-Gonzalez, A.; Willson, M.; Wirnsberger, P.; Fortunato, M.; Alet, F.; Ravuri, S.; Ewalds, T.; Eaton-Rosen, Z.; Hu, W.; et al. Learning skillful medium-range global weather forecasting. *Science* **2023**, *382*, 1416–1421. [[CrossRef](#)]
82. Selz, T.; Craig, G.C. Can artificial intelligence-based weather prediction models simulate the butterfly effect? *Geophys. Res. Lett.* **2023**, *50*, e2023GL105747. [[CrossRef](#)]
83. Watt-Meyer, O.; Dresdner, G.; McGibbon, J.; Clark, S.K.; Henn, B.; Duncan, J.; Brenowitz, N.D.; Kashinath, K.; Pritchard, M.S.; Bonev, B.; et al. ACE: A fast, skillful learned global atmospheric model for climate prediction. *arXiv* **2023**, arXiv:2310.02074v1. [[CrossRef](#)]
84. Bach, E.; Krishnamurthy, V.; Mote, S.; Shukla, J.; Sharma, A.S.; Kalnay, E.; Ghil, M. Improved subseasonal prediction of South Asian monsoon rainfall using data-driven forecasts of oscillatory modes. *Proc. Natl. Acad. Sci. USA* **2024**, *121*, e2312573121. [[CrossRef](#)] [[PubMed](#)]
85. Bouallègue, Z.B.; Clare, M.C.A.; Magnusson, L.; Gascón, E.; Maier-Gerber, M.; Janoušek, M.; Rodwell, M.; Pinault, F.; Dramsch, J.S.; Lang, S.T.K.; et al. The rise of data-driven weather forecasting: A first statistical assessment of machine learning-based weather forecasts in an operational-like context. *Bull. Am. Meteorol. Soc.* **2024**, *105*, E864–E883. [[CrossRef](#)]
86. Li, H.; Chen, L.; Zhong, X.; Wu, J.; Chen, D.; Xie, S.P.; Chao, Q.; Lin, C.; Hu, Z.; Lu, B.; et al. A machine learning model that outperforms conventional global subseasonal forecast models. *Phys. Sci.* **2024**, under review. [[CrossRef](#)]
87. Hersbach, H.; Bell, B.; Berrisford, P.; Biavati, G.; Horányi, A.; Muñoz Sabater, J.; Nicolas, J.; Peubey, C.; Radu, R.; Rozum, I.; et al. ERA5 hourly data on single levels from 1979 to present. *Copernic. Clim. Change Serv. (C3S) Clim. Data Store (CDS)* **2018**, *10*.
88. Hersbach, H.; Bell, B.; Berrisford, P.; Hirahara, S.; Horányi, A.; Muñoz-Sabater, J.; Nicolas, J.; Peubey, C.; Radu, R.; Schepers, D.; et al. The ERA5 Global Reanalysis. *Q. J. R. Meteorol. Soc.* **2020**, *146*, 1999–2049. [[CrossRef](#)]
89. Eyring, V.; Bony, S.; Meehl, G.A.; Senior, C.A.; Stevens, B.; Stouffer, R.J.; Taylor, K.E. Overview of the coupled model intercomparison project phase 6 (CMIP6) experimental design and organization. *Geosci. Model Dev.* **2016**, *9*, 1937–1958. [[CrossRef](#)]
90. Vaswani, A.; Shazeer, N.; Parmar, N.; Uszkoreit, J.; Jones, L.; Gomez, A.N.; Kaiser, Ł.; Polosukhin, I. “Attention Is All You Need”. In *Advances in Neural Information Processing Systems*; Curran Associates, Inc.: Red Hook, NY, USA, 2017; Volume 30, Available online: <https://proceedings.neurips.cc/paper/2017/file/3f5ee243547dee91fbd053c1c4a845aa-Paper.pdf> (accessed on 1 May 2024).
91. Dosovitskiy, A.; Beyer, L.; Kolesnikov, A.; Weissenborn, D.; Zhai, X.; Unterthiner, T.; Dehghani, M.; Minderer, M.; Heigold, G.; Gelly, S.; et al. An Image is Worth 16x16 Words: Transformers for Image Recognition at Scale. *arXiv* **2020**, arXiv:2010.11929. [[CrossRef](#)]
92. Bodnar, C.; Bruinsma, W.P.; Lucic, A.; Stanley, M.; Brandstetter, J.; Garvan, P.; Riechert, M.; Weyn, J.; Dong, H.; Vaughan, A.; et al. Aurora: A Foundation Model of the Atmosphere. *arXiv* **2024**, arXiv:2405.13063. [[CrossRef](#)]
93. Kochkov, D.; Yuval, J.; Langmore, I.; Norgaard, P.; Smith, J.; Mooers, G.; Lottes, J.; Rasp, S.; Düben, P.; Klöwer, M.; et al. Neural General Circulation Models for Weather and Climate. *arXiv* **2024**, arXiv:2311.07222. [[CrossRef](#)]
94. Lang, S.; Alexe, M.; Chantry, M.; Dramsch, J.; Pinault, F.; Raoult, B.; Clare, M.C.; Lessig, C.; Maier-Gerber, M.; Magnusson, L.; et al. AIFS—ECMWF’S Data-Driven Forecasting System. *arXiv* **2024**, arXiv:2406.01465. [[CrossRef](#)]
95. Mardani, M.; Brenowitz, N.; Cohen, Y.; Pathak, J.; Chen, C.Y.; Liu, C.C.; Vahdat, A.; Kashinath, K.; Kautz, J.; Pritchard, M. Residual Diffusion Modeling for Km-scale Atmospheric Downscaling. *arXiv* **2023**, arXiv:2309.15214. [[CrossRef](#)]
96. Price, I.; Sanchez-Gonzalez, A.; Alet, F.; Ewalds, T.; El-Kadi, A.; Stott, J.; Mohamed, S.; Battaglia, P.; Lam, R.; Willson, M. 2024: GenCast: Diffusion-based ensemble forecasting for medium-range weather. *arXiv* **2023**, arXiv:2312.15796. [[CrossRef](#)]
97. Vonich, P.T.; Hakim, G.J. Predictability Limit of the 2021 Pacific Northwest Heatwave from Deep-Learning Sensitivity Analysis. *arXiv* **2024**, arXiv:2406.05019. [[CrossRef](#)]
98. Wu, Y.; Xue, W. Data-Driven Weather Forecasting and Climate Modeling from the Perspective of Development. *Atmosphere* **2024**, *15*, 689. [[CrossRef](#)]
99. Shen, B.-W. Aggregated negative feedback in a generalized Lorenz model. *Int. J. Bifurc. Chaos* **2019**, *29*, 1950037. [[CrossRef](#)]
100. Shen, B.-W.; Reyes, T.; Faghieh-Naini, S. Coexistence of Chaotic and Non-Chaotic Orbits in a New Nine-Dimensional Lorenz Model. In *11th Chaotic Modeling and Simulation International Conference*; CHAOS 2018; Skiadas, C., Lubashevsky, I., Eds.; Springer Proceedings in Complexity; Springer: Cham, Switzerland, 2019. [[CrossRef](#)]
101. Zeng, X. Atmospheric Instability and Its Associated Oscillations in the Tropics. *Atmosphere* **2023**, *14*, 433. [[CrossRef](#)]
102. Shen, B.-W.; Pielke, R.A., Sr.; Zeng, X. Special Issue Theme Topic: “Revisiting Butterfly Effect, Multiscale Dynamics, and Predictability Using Ai-Enhanced Modeling Framework (AEMF) and Chaos Theory”. 2024. Available online: <https://www.mdpi.com/topics/B9N0115Q3E> (accessed on 1 May 2024).
103. Atlas, R.; Reale, O.; Shen, B.; Lin, S.; Chern, J.; Putman, W.; Lee, T.; Yeh, K.; Bosilovich, M.; Radakovich, J. Hurricane forecasting with the high-resolution NASA finite-volume General Circulation Model. *Geophys. Res. Lett.* **2005**, *32*, L03801. [[CrossRef](#)]
104. Shen, B.-W.; Atlas, R.; Oreale, O.; Lin, S.-J.; Chern, J.-D.; Chang, J.; Henze, C.; Li, J.-L. Hurricane Forecasts with a Global Mesoscale-Resolving Model: Preliminary Results with Hurricane Katrina (2005). *Geophys. Res. Lett.* **2006**, *33*, L13813. [[CrossRef](#)]
105. Shen, B.-W.; Atlas, R.; Chern, J.-D.; Reale, O.; Lin, S.-J.; Lee, T.; Chang, J. The 0.125 degree Finite Volume General Mesoscale Circulation Model: Preliminary simulations of mesoscale vortices. *Geophys. Res. Lett.* **2006**, *33*, L05801. [[CrossRef](#)]
106. Paxson, W.; Shen, B.-W. A KdV-SIR Equation and Its Analytical Solutions for Solitary Epidemic Waves. *Int. J. Bifurc. Chaos* **2022**, *32*, 2250199. [[CrossRef](#)]

107. Reynolds, C.A.; Webster, P.J.; Kalnay, E. Random error growth in NMC's global forecasts. *Mon. Weather Rev.* **1994**, *122*, 1281–1305. [[CrossRef](#)]
108. Kalnay, E. *Atmospheric Modeling, Data Assimilation and Predictability*; Cambridge University Press: Cambridge, UK, 2002. [[CrossRef](#)]
109. Shen, B.-W.; Pielke, R.A., Sr.; Zeng, X.; Baik, J.-J.; Faghieh-Naini, S.; Cui, J.; Atlas, R.; Reyes, T.A. Is Weather Chaotic? Coexisting Chaotic and Non-Chaotic Attractors within Lorenz Models. In Proceedings of the 13th Chaos International Conference CHAOS 2020, Florence, Italy, 9–12 June 2020; Skiadas, C.H., Dimotikalis, Y., Eds.; Springer Proceedings in Complexity. Springer: Cham, Switzerland, 2021.

Disclaimer/Publisher's Note: The statements, opinions and data contained in all publications are solely those of the individual author(s) and contributor(s) and not of MDPI and/or the editor(s). MDPI and/or the editor(s) disclaim responsibility for any injury to people or property resulting from any ideas, methods, instructions or products referred to in the content.